Serum response factor orchestrates nascent sarcomerogenesis and silences the biomineralization gene program in the heart

Zhiyv Niu[a,b], Dinakar Iyer[c], Simon J. Conway[d], James F. Martin[e], Kathryn Ivey[f], Deepak Srivastava[f], Alfred Nordheim[g], and Robert J. Schwartz[e,1]

[a]Center for Cardiovascular Development, [b]Section of Cardiovascular Sciences, and [c]Department of Medicine, Baylor College of Medicine, Houston, TX 77030; [d]Cardiovascular Development Group, Herman B. Wells Center for Pediatric Research, Indiana University School of Medicine, Indianapolis, IN 46202; [e]Center for Molecular Development and Disease, Institute of Biosciences and Technology, Texas A&M University System Health Science Center, Houston, TX 77030; [f]Gladstone Institute of Cardiovascular Disease, San Francisco, CA 94158; and [g]Institute of Molecular Biology, Tuebingen University, D-72704 Tuebingen, Germany

Edited by Eric N. Olson, University of Texas Southwestern Medical Center, Dallas, TX, and approved September 18, 2008 (received for review June 6, 2008)

Our conditional serum response factor (SRF) knockout, Srf^{Cko}, in the heart-forming region blocked the appearance of rhythmic beating myocytes, one of the earliest cardiac defects caused by the ablation of a cardiac-enriched transcription factor. The appearance of Hand1 and Smyd1, transcription and chromatin remodeling factors; Acta1, Acta2, Myl3, and Myom1, myofibril proteins; and calcium-activated potassium-channel gene activity (KCNMB1), the channel protein, were powerfully attenuated in the Srf^{CKO} mutant hearts. A requisite role for combinatorial cofactor interactions with SRF, as a major determinant for regulating the appearance of organized sarcomeres, was shown by viral rescue of SRF-null ES cells with SRF point mutants that block cofactor interactions. In the absence of SRF genes associated with biomineralization, GATA-6, bone morphogenetic protein 4 (BMP4), and periostin were strongly up-regulated, coinciding with the down regulation of many SRF dependent microRNA, including miR1, which exerted robust silencer activity over the induction of GATA-6 leading to the down regulation of BMP4 and periostin.

heart development | microRNA | periostin | cardiogenesis | GATA6

The heart is the first organ to form in mammals, controlled by an exquisite program that results in the assembly of organized sarcomeres that rhythmically beat. First, molecular principles underlying sarcomerogenesis were based on the gene-switch paradigm in which nonmuscle actins are replaced by smooth muscle and cardiac α-actins in the heart-forming region (1, 2). Serum response factor (SRF), identified by Treisman and colleagues (3), and a MADS (MCM1, Agamous, Deficiens, serum response factor) box transcription factor may play a critical role in sarcomerogenesis, as deduced from transfection assays demonstrating the essential role of SRF binding sites, or CArG boxes, for switching on cardiac gene transcription, competition with negative acting YY1 and HOP, and cardiac restricted expression (reviewed in ref. 4). Cardiac progenitors receiving the appropriate developmental cues switch on several cardiac-restricted transcription factors such as Nkx2–5, GATA-4, and myocardin that interact with SRF to activate many cardiac and smooth-muscle structural genes (reviewed in refs. 4, 5). SRF target genes are also involved with contractility, cell movement, and cell growth signaling (6, 7) and the recently discovered microRNAs, required for normal heart development (8).

The function of SRF in heart development in vivo has been obscured by the early lethality of SRF null mice before the onset of cardiogenesis (9). Even recent SRF inactivation studies in the heart, performed through a conditional knockout strategy by using Cre recombinase driven by late expressing transgenic promoters such as, SM22α, and or α/β myosin-heavy chains, failed to reveal an obligatory role for SRF in controlling the appearance of beating myocytes (10–12). That failure is because SRF induced during early cardiogenesis is relatively stable and sarcomeres appeared even after Cre recombinase mediated ablation of the SRF genetic locus (12). To dissect out SRF's role during early cardiac myocyte commitment and differentiation, we generated lineage-specific deletion of SRF with our $Nkx2.5^{Cre}$ (13) and $Srf^{LoxP/Loxp}$ mice (14) in the HFR, well before SRF protein actually accumulated in the heart.

Results

The SRF Cardiac-Null Mutant Exhibited Nonbeating and Heart-Looping Defect. To block the appearance of SRF before the appearance of beating cardiac myocytes, we engineered a mouse that carried both Srf^{LacZ} and $Nkx2.5^{Cre}$ on chromosome 17 which was then bred to $SRF^{Lox/Lox}$ mice to generate a conditional SRF knockout (Srf^{Cko}) in the heart-forming region. The Srf^{Cko} mutant genotyped as $Srf^{LacZ/Flox}$:$Nkx2.5Cre$ was first discernible at approximately 8.0 dpc (linear heart-tube stage) with a nonbeating heart tube (Fig. 1*A*). Immunofluorescence staining with anti-SRF antibodies showed SRF staining in myocytes of haploid SRF mutant embryos and the absence of SRF in the Srf^{Cko} embryo (Fig. 1 *B–E*). This tubular structure misplaced the anterior portion of the developing out-flow tract in the Srf^{Cko} mutant (Fig. 1 *F* and *G*). By ≈8.5 dpc, severe ventricular dilation and cranially retained right ventricle/outflow tract were 2 common morphological defects of this motionless tubular heart (Fig. 1 *H* and *I*) The outflow tract derived from second heart field (SHF) was undersized, as shown by Wnt11 expression (Fig. 1 *J* and *K*, ref. 15), whereas cardiac field-marker genes *Nkx2.5* (16) and *Fgf10* (17) appeared unaffected (Fig. 1 *L–O*).

SRF Guides Cardiac Myogenesis. Smooth muscle and cardiac α-actin gene RNA transcripts emerging at the late cardiac-crescent stage (7.75–8.0 dpc) were blocked in Srf^{Cko} mutant hearts (Fig. 2 *A–H*). Immunofluorescence staining confirmed the absence of smooth muscle and striated α-actin in the hearts of Srf^{Cko} embryos (Fig. 2 *C*, *D*, *G*, and *H*). Expression of *Myl2* and *Myom1* components of the thick filament and M-band of sarcomeres were dependent on SRF expression (Fig. 2 *I–L*). Analysis with transmission electron micros-

Author contributions: Z.N., D.I., S.J.C., J.F.M., K.I., D.S., and R.J.S. designed research; Z.N., D.I., S.J.C., J.F.M., and K.I. performed research; A.N. contributed new reagents/analytic tools; Z.N., D.I., S.J.C., J.F.M., K.I., D.S., and R.J.S. analyzed data; and Z.N. and R.J.S. wrote the paper.

The authors declare no conflict of interest.

This article is a PNAS Direct Submission.

[1]To whom correspondence should be addressed. E- mail: rschwartz@ibt.tamhsc.edu.

This article contains supporting information online at www.pnas.org/cgi/content/full/0805491105/DCSupplemental.

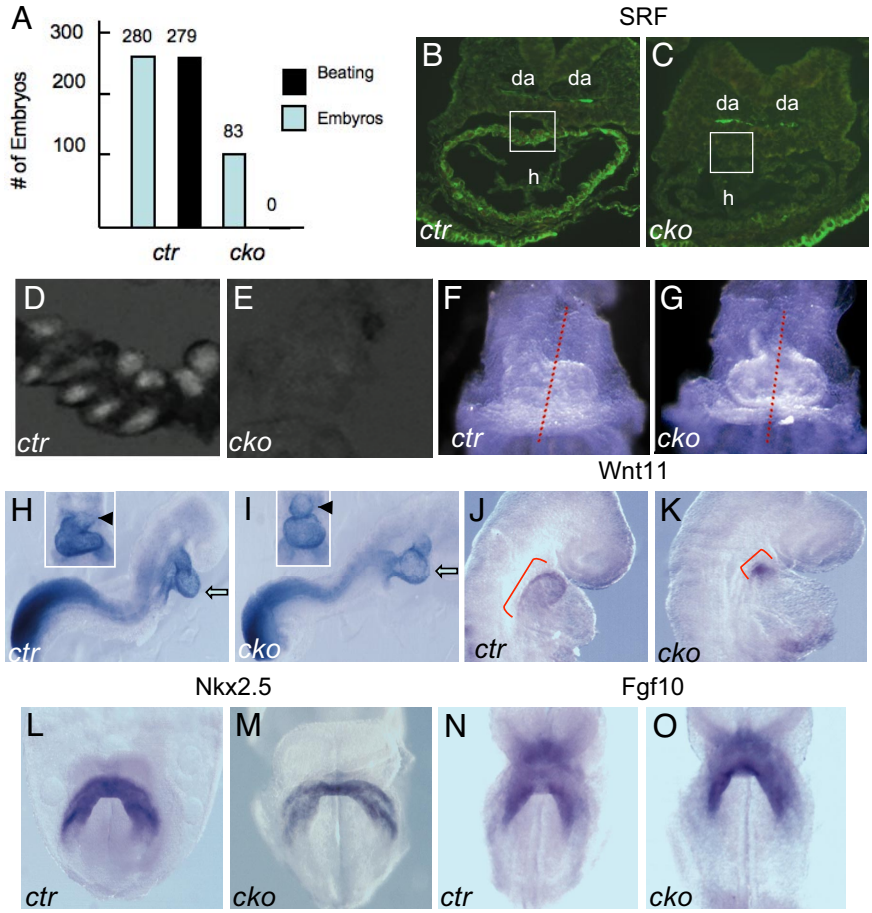

Fig. 1. Early cardiac restricted *Srf* knockout exhibited nonbeating and cardiac looping defects. (*A*) Quantitative summary of the number of beating hearts observed for control and Srf^{Cko} embryos at ≈8.25 dpc. (*B–E*) Immunofluorescent staining of control $Srf^{Lox/+}$ and Srf^{Cko} embryo sections anti-SRF (green) antibodies. Boxed areas in *B* and *C* were magnified in panels *D* and *E*. (*F–I*) Control (*ctr*) $Srf^{Lox/+}$ and Srf^{Cko} embryos at ≈8.25 dpc. Cardiac looping was affected in Srf^{cko} embryo. Red dashed line, body middle line. Whole mount lacZ staining revealed the right ventricle and outflow tract (arrow head) and the dilated left ventricle (open arrow) in Srf^{Cko} embryo. (*J* and *K*) Reduced Wnt11 RNA transcripts in the Srf^{Cko} embryo indicated an undersized outflow tract and a SHF at 7.75 dpc. (*L–O*) The first heart field appeared unaffected, as shown by the similar levels of *Nkx2.5* and *Fgf10* RNA transcripts in both the control and Srf^{Cko} embryo at 7.75 dpc.

copy indicated that neither aligned filaments nor Z disks that were formed in multiple Srf^{Cko} cardiac mutants correlated well with the nonbeating heart (Fig. 2 *M–Q*). These "paralyzed" mutant hearts did not display any sarcomere signatures in multiple Srf^{Cko} mutant samples.

The appearance of *Smyd1*, a cardiac and skeletal muscle-specific chromatin-remodeling factor (18) failed to appear in the nascent Srf^{Cko} mutant myocytes (Fig. 3 *A* and *B*). Expression of Tgf1/1, a LIM protein that serves as a cofactor with the androgen receptor and p300 (19), was also blocked in the

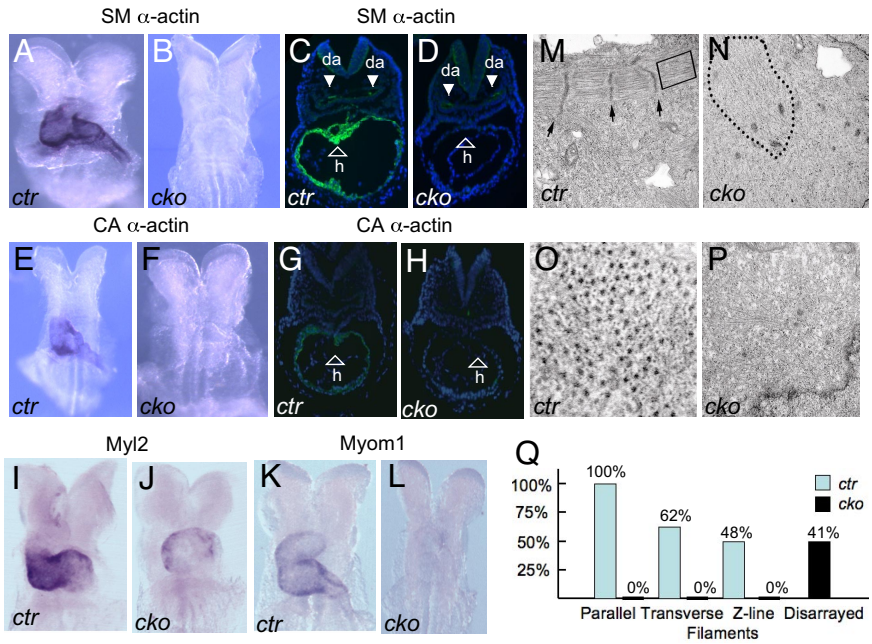

Fig. 2. SRF insufficiency shuts down cardiac myocyte differentiation. (*A–H*) Whole mount in situ hybridization and immunofluorescence staining showed the absence of *Acta2* (smooth muscle α-actin) and *Actc1* (cardiac α-actin) expression in the Srf^{Cko} embryo in comparison to control embryos at 8.5 dpc. (*I–L*) Whole mount in situ hybridization showed down-regulation of *Myl2* and *Myom1* in Srf^{Cko} embryos. (*M–P*) Transmission EM revealed organized sarcomere structure in control (*M* and *O*) but not Srf^{Cko} sections (*N* and *P*). (*Q*) Quantitative summary of contractile structures recognized in multiple control and Srf^{Cko} samples. In control samples (*M* and *O*) Z-lines were observed at high incidence (n = 10:21 myocytes), whereas aligned filament bundles were observed in all control samples. "Disarrayed" filament structures shown within the dotted lines were observed in less than half of the Srf^{cko} mutant cells (n = 11:27 cells) which shared a diameter at 10 nm, same as noncontractile intermediated filaments (*N* and *P*).

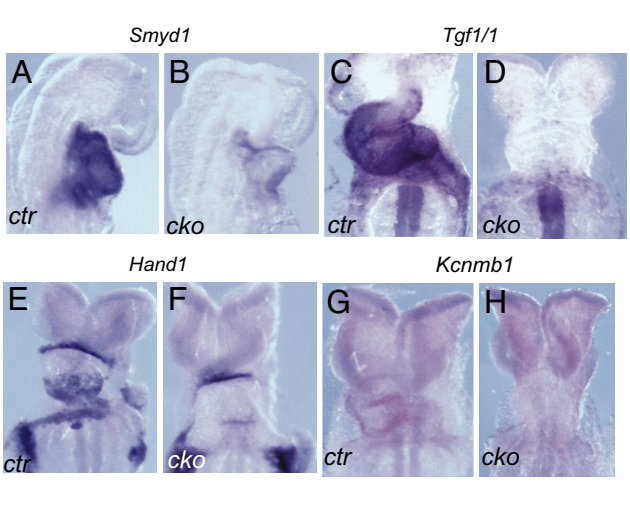

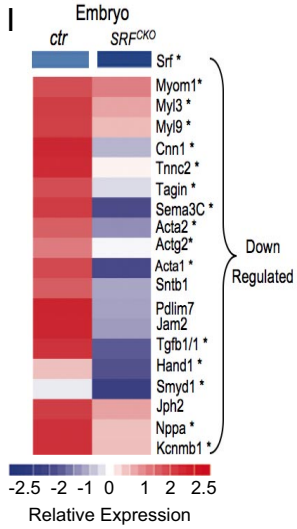

Fig. 3. Identification of novel SRF downstream target genes important for sarcomerogenesis and electrical coupling. (*A* and *B*) Whole mount in situ hybridization of Smyd1, (*C* and *D*) Tgf1/1, (*E* and *F*) Hand 1, (*G* and *H*) KCNMB1 showed reduced expression of these genes in Srf^{Cko} embryos in comparison to control $Srf^{+/lox}$ embryos at ≈8.5 dpc. (*I*) RNA samples isolated from control and SRF^{Cko} mutant embryonic hearts were hybridized against Affymetrix array 430a2 chip. Microarray raw data analysis was done with dCHIP software (www.dchip.org). Note the down-regulation of SRF gene targets. Genome TraFac searched putative SRF binding motifs 5 kb upstream to the 1st exon, and motifs displaying above 70% similarity between human and murine genome were noted by asterisks.

Srf^{Cko} mutant heart (Fig. 3 *C* and *D*). Expression of the *Hand1* gene, a first heart-field maker, was reduced in the Srf^{Cko} mutant (Fig. 3 *E* and *F*), and may have also contributed to ventricular dilation. Appearance of calcium-activated potassium-channel gene activity (KCNMB1) was blunted in the Srf^{Cko} mutant hearts (Fig. 3 *G* and *H*). Many of these genes were validated for the presence of conserved CArG elements in their promoters (Fig. 3*I*).

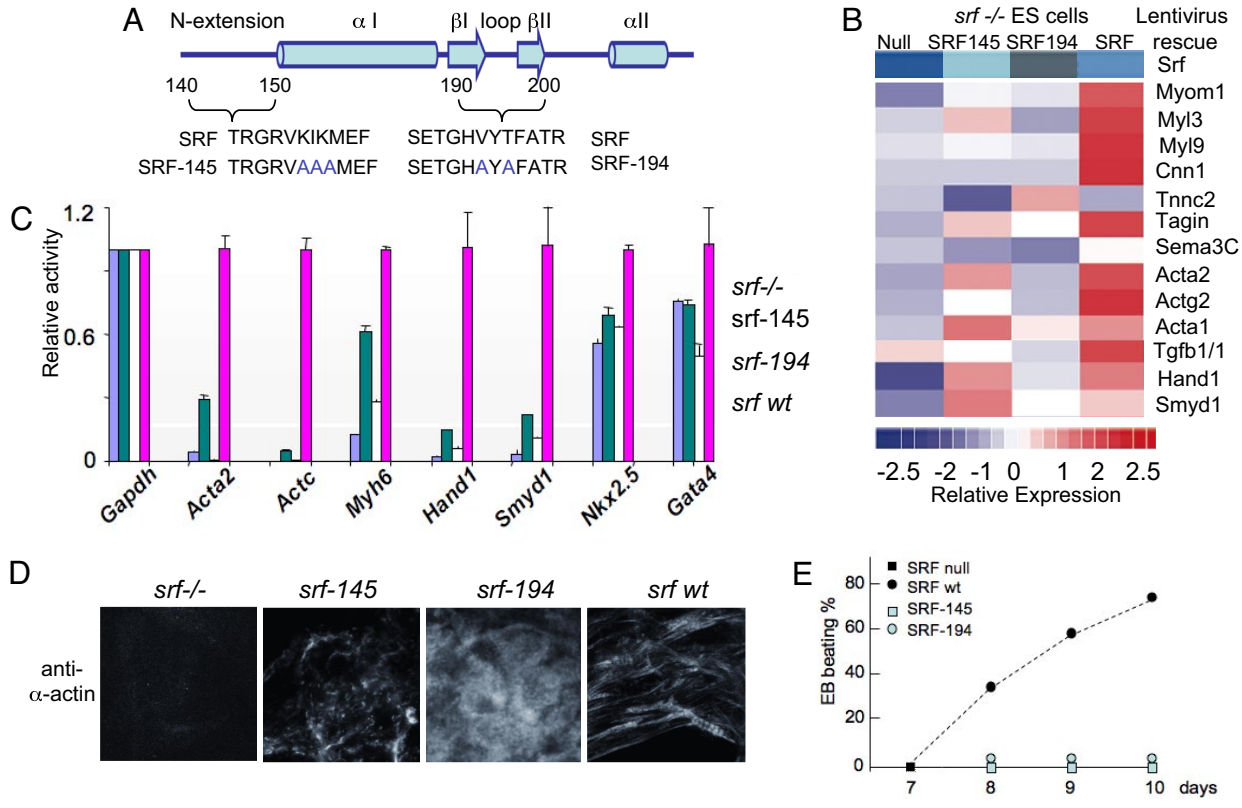

Fig. 4. Rescue of cardiac myogenic differentiation defect in *Srf* -null ES cells by SRF wild-type and interaction defective mutants reveal an obligatory role for SRF and cofactor interactions to drive sarcomerogenesis and contractility. (*A*) SRF contains an evolutionary conserved MADS box domain that allows for dimerization of SRF monomers and DNA binding to a CArG element. This diagram shows the N-extension, alpha I coil, beta I sheet, beta-loop, beta II sheet, and alpha II coil of the SRF-DNA crystal structure adapted from Pellegrini *et al*. (37). Alanine substitution mutations were made in the MADS box at amino acids 145–147 (SRF-145) and at amino acids 194 and 196 (SRF-194). (*B*) Affymetrix expression microarray showed a subset of genes that were consistently affected by the lentiviral rescue of SRF-null ES cells with wild-type SRF during embryoid body formation leading to cardiac cell differentiation. (*C*) Quantitative RT-PCR showing the effects of the rescue of *Srf*-null ES cells with lentiviruses expressing SRF wild-type and SRF point mutants on the expression of SRF targets, which included *Acta2*, *Actc1*, *Myh6*, *Hand1*, *Smyd1*, and cardiac regulatory factors *Nkx2.5* and *Gata4*. (*D*) Immunofluorescent detection of sarcomeric α-actin following lentivirus mediated infection and expression of SRF and point mutants SRF-145 and SRF-194 in $Srf^{-/-}$ ES cell. (*E*) Beating embryoid bodies were found only in *Srf*-null ES cells rescued by lentiviral infection with SRF wild type.

SRF Mutants Block Sarcomerogenesis in *Srf*-null ES Cells. The idea that SRF activity is largely controlled by its interaction with cofactors was tested by a "gain-of-function" approach applied to *Srf*-null ES cells. We focused on two mutants: SRF-145 (triple alanine substitutions 145–147 amino acids) and SRF-194 (dual alanine substitutions at 194 and 196 amino acids; Fig. 4*A*. These two mutants did not interfere with DNA binding, but prevented their coassociation and facilitated binding of SRF with Nkx2.5/GATA4 (SRF-145 mutant), or myocardin [SRF-194 mutant; supporting information (SI) Fig. S1]. Increased expression of wild-type SRF and mutants by the lentivirus system was sufficient to either rescue completely and or in part the cardiac myogenesis defect of $Srf^{-/-}$ ES cells (Fig. 4 *B–D*). Microarray analysis and quantitative RT-PCR confirmed the rescue and enhanced expression of Hand1 and Smyd1, transcription and chromatin remodeling factors, Acta1, Acta2, Myl3, and Myom1, myofibril proteins, and *Kcnmb1* excitation contraction coupling proteins by SRF replenishment in $Srf^{-/-}$ ES cells (Fig. 4 *B* and *C*). Measurement of GATA4, myocardin, and MRTFs transcripts indicated that there were sufficient amounts of these factors to allow for gene activation in the presence of the SRF mutants (Fig. S2). Moderate elevation of some structural gene expression was elicited by either SRF-145 or SRF-194, but neither mutant alone was sufficient to drive terminal cardiac myocyte differentiation, as determined by immunofluorescent staining of organized sarcomeres, microarray analysis, and beating cardiac myocytes (Fig. 4 *D* and *E*, and Movies S1–S4). Given the fact that SRF directed the appearance of beating myocytes from SRF-null ES cells, we conclude that the inability of the SRF interaction-defective mutants to rescue myogeneis highlighted the significance of these cofactor associations in cardiac myogenesis and not their absence.

SRF, a Biomineral and Extracellular Gene Program Silencer. Analysis of cardiac Srf^{Cko} also revealed strong up-regulation of GATA-6, bone morphogenetic protein 4 (BMP4), and periostin (Postn) genes associated with biomineral formation (Fig. 5*A*), in the regions of the endocardium destined to become the septum and outflow tract and the SHF (Fig. 5 *B–G*). Postn is expressed in the mesenchymal-derived cardiac fibroblasts, valvular attachment apparatus, and epicardial/pericardial structures, but is absent from the cardiomyocyte lineage (20). Expression of BMPs in the myocardium is critical for the induction of Postn (21). *mef2c-AHF-Cre* transgenic mice were used to direct the expression of Cre recombinase exclusively in the anterior heart field and its derivatives to conditionally ablate the $Bmp4^{Lox/Lox}$ gene. Endothelial and myocardial components of the outflow tract, right ventricle, and ventricular septum were shown to be derivatives of mef2c-AHF-Cre expressing cells (22). The *mef2c-AHF-Cre* transgene-induced knockout of $Bmp4^{Lox/Lox}$ in the E10.5 mouse embryonic-mouse heart blocked the appearance of Postn in the outflow tract (Fig. 5 *H* and *I*). In addition, closely related BMP-2 induced periostin expression in cardiac-cushion mesenchymal cells (21), thus support the role of BMP signaling, leading to periostin expression.

Periostin may also suppress myocyte differentiation. Conversely, periostin deletion might result in enhanced and/or ectopic myocyte differentiation. To distinguish the appearance of cardiomyocytes from the *Postn*-expressing noncontractile tissues, we made use of the *αMHC-EGFP* reporter mice (23) that express EGFP exclusively in cardiac muscle in the background of targeted-null ($Postn^{LacZ}$) neonatal mice. Surviving adult $Postn^{LacZ}$-null hearts contained ectopic αMHC^{EGFP} expression, as EGFP-positive islands in the null epicardium (n = 9:13 $Postn^{LacZ}$ null αMHC^{EGFP} hearts examined; Fig. 5*J*). This was confirmed via costaining with the myocardial-marker MF20 in $Postn^{LacZ}$ null, but not wild-type, epicardium (not shown).

SRF Directs the Expression of Many MicroRNAs Including miR1. SRF may exert gene silencing activities through its regulation over

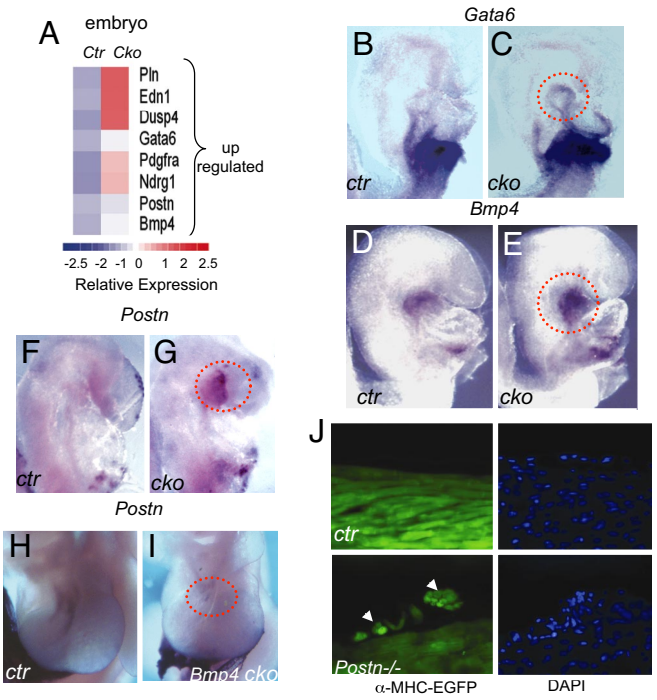

Fig. 5. Activation of biomineralization markers observed in Srf^{Cko} mutant hearts. (*A*) dCHIP analysis of prominent genes up-regulated in the Srf^{Cko} embryo. Whole mount in situ hybridization of (*B* and *C*) Gata6, (*D* and *E*) BMP4, and (*F* and *G*) Postn showed elevated expression of these genes in Srf^{Cko} embryos in comparison to control $Srf^{Lox/+}$ embryos at approximately 8.5 dpc. (*H* and *I*). Whole mount in situ hybridization showed induced expression of *Postn* in the Bmp4Cko heart in comparison to the control $Bmp4^{Lox/+}$:$Mef2C^{Cre}$ heart. (*J*) Ectopic appearance of cardiac myocytes (white arrow head, tg-α-MHC-eGFP positive) identified in epicardium layer of the *Postn*-null heart.

microRNAs (miRNAs). In day 9.5 Srf^{Cko} embryonic-mutant hearts, ≤20 miRNAs, each of which contain at least 1 conserved CArG element in their promoters, were down-regulated in comparison to control heart samples (Fig. 6*A*). Among these miRNAs, miR-1 (8) was shown to be controlled by SRF through its 3 CArG boxes (24). In addition, mice lacking miR-1–2 have a spectrum of cardiac abnormalities also allowed for the induction of GATA-6 (8). Greater than 90% of miR-1 RNA transcripts were blocked in the Srf^{Cko} hearts, whereas GATA6 mRNA levels increased over 18 fold (Fig. 6 *B* and *C*). Thus, tissue-specific expression of miRNAs regulated by SRF at the transcriptional level may have a strong regulatory activity over the noncontractile endocardial/epicardial gene activity.

miR-1 Blocked GATA6 and Periostin Expression. To test this idea, we evaluated the role of SRF in regulation of miR-1 in the SRF lentiviral rescue of *Srf*-null ES cells (Fig. 6). Viral-expressed SRF induced about a 30-fold increase in miR-1 RNA, as shown by quantitative RT PCR analysis (Fig. 6*D*). We observed increased levels of GATA6 (BMP2:4; data not shown) and periostin in *Srf*-null ES cells, and stable transfectants of these ES cells with miR-1 significantly repressed GATA6 and Postn expression, whereas miR-133, the miR-1 bicistronic partner, failed to inhibit their expression (Fig. 6 *E* and *F*). Of the key biomineralization genes, only the well-conserved sites in mouse and rat GATA6 3′UTR, are favorably accessible, according to the algorithm reported by Zhao *et al.* (8; (Fig. S3). MiR-1 sites were not detected in Postn; thus, miR1 indirectly influenced Postn expression most likely through the silencing of GATA6.

DEVELOPMENTAL BIOLOGY

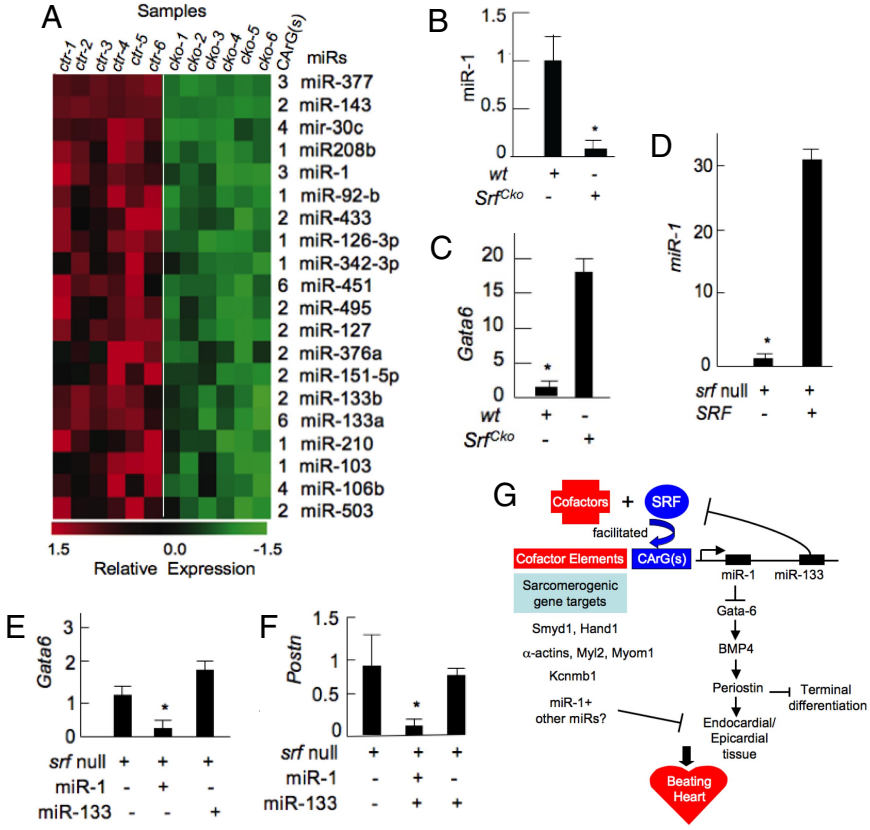

Fig. 6. Regulation of SRF-dependent microRNA and miR-1 targets. (*A*) Microarray analysis of SRF-dependent microRNAs that were down-regulated in the srf^{cko}-mutant hearts. Genome-wide microRNA expression profiling was accomplished with RNA samples taken from control and SRF^{CKO}-mutant hearts and hybridized on a mouse microRNA microarray platform (MRA-1002, LC Sciences) contained 568 unique mature miRNA sequences. (*B*) Quantitative RT-PCR showed down-regulation of miR-1 (including miR-1–1 and miR-1–2) in RNA taken from SRF^{CKO}-mutant hearts in comparison to control samples. (*C*) Quantitative RT-PCR showed up-regulation of Gata6 in Srf^{cko}-embryo heart samples. (*D*). Quantitative RT-PCR showed rescue of $Srf^{-/-}$ ES cells with lentviral expression of SRF, as shown in Fig. 4, strongly induced miR-1 RNA transcripts. (*E* and *F*) Quantitative RT-PCR showed that stable transfectants of miR-1, but not miR-133, its bicistronic partner, in $Srf^{-/-}$ ES cells blocked the expression of GATA6 and periostin. (*G*) Schematic diagram shows the role of SRF and cofactors in regulating sarcomeric downstream targets that includes coding and noncoding microRNA. SRF cofactors facilitate SRF binding to promoters that drive the expression of heart restricted transcription factors, sarcomeric contractile proteins, ion channels, and the 20 miRNAs which were shown as downstream targets of SRF. This diagram also summarizes the roles of the SRF dependent miR1 silencing of the GATA6, BMP4, and periostin dependent biomineralization and connective tissue expression gene activity and miR133 inhibiting SRF expression.

Discussion

SRF Orchestrates Cardiac Myogenesis Through Multiple Levels of Regulation. Our study provides inconvertible evidence that SRF activity controls sarcomerogenesis in higher vertebrates, as modeled in the schematic diagram in Fig. 6*G*. Recently, Fukushige *et al*., (25) demonstrated that UNC-120, the *C. elegans* equivalent of SRF, was required to initiate a body-wall muscle program in naive early blastomeres and to drive muscle-structural gene activity. The *unc-120*-null mutants exhibited low-level myofilament protein production. The ability for SRF to be the universal "myogenic driver" was totally abrogated in the *Srf*-null cells and supports the concept that SRF resides at a high point in the regulatory hierarchy governing sarcomerogenesis from worms to mammals. Additionally, SRF activity was also controlled to a large extent through combinatorial factor interactions with tissue-specific regulatory cofactors and was supported by our rescue of *Srf* null ES cells with lentiviral-expressed SRF-point mutants that blocked co-factor association, but not DNA binding activity. Because SRF mutants were incapable of restoring sarcomerogenesis, our data supports the claim that SRF plays an obligatory role in cardiac myogenesis with a requirement for SRF cofactor interactions.

In the absence of *Srf*, we observed the strong up-regulation of biomineral and extracellular matrix-gene activity. GATA6 contributes to septal and valvular development via its direct transcription target, BMP4, leading the induction of Postn (26). The deletion of the BMP type 1A receptor in the endocardium also resulted in failed cushion formation, indicating that BMP signals directly to cushion-forming endocardium to induce epithelial-mesenchyme transition (27). Transformation of atrioventricular (AV) canal endocardium into invasive mesenchyme correlates spatially and temporally with the expression of BMPs in the atrioventricular myocardium crucial for the induction of Postn (28). Kühn *et al*. (29) showed that periostin-induced cardiomyocyte cell-cycle reentry and mitosis, whereas periostin expression was associated with improved ventricular remodeling and myocardial function (30). We showed that conditional abrogation of periostin by targeted gene-deletion-activated cardiac-cell differentiation, as exemplified by the ectopic expression of the αMHC^{EGFP}-fluorescent gene reporter (Fig. 5).

SRF, a Powerful Silencer Directs the Expression of Many miRNAs, Including miR-1. SRF may also direct the expression of many miRs that inhibit the expression of cardiac regulatory factors that influence cardiac lineage specification. Twenty miRs were significantly down-regulated in the SRF^{Cko}-mutant heart (Fig. 5*A*). As shown here, miR-1 RNA transcripts were dependent upon SRF expression and were blocked in Srf^{Cko} hearts. Rescue of SRF-null ES cells with viral expressed SRF induced ≈thirty-fold increase in miR-1 RNA (Fig. 6). Increased levels of GATA6 and Postn in *Srf*-null ES cells were also attenuated by miR-1, but not by miR-133, the miR-1 bicistronic partner. Thus, miR-1 appears to play an important role in regulating GATA6 expression leading to endocardial/epicardial gene silencing. In addition, Chen *et al*. (31) showed that expression of miR-133 repressed myoblast differentiation by repressing SRF expression. Thus, miR-133 is controlled by SRF, yet directs a negative regulatory loop through inhibiting SRF translation (Fig. 6*G*). Possibly, the delicate balance of SRF-directed silencing of miRNA activity may be even more profound in human heart disease. Chang *et al*. (32) found SRF was cleaved by caspase 3 in human heart failure and generated its dominant-negative SRF-N in the failing human myocardium. Thus, during the onset of heart failure, cleaved SRF will likely interfere with SRF's global role in controlling genes required for sarcomerogenesis, but may also hinder the expression of SRF-dependent miRNAs that silence gene activities causing dysregulation of normal cardiac performance.

Experimental Procedures

Generation of SRF Cardiac Progenitor-Conditional Null Embryos and Transient Transgenics. The SRF LacZ "knock-in" mouse $SRF^{LacZ/+}$ (33) and the Cre-conditional $SRF^{LoxP/LoxP}$ mouse (13) were previously generated. Cardiac progen-

itor-specific Cre-recombinase transgenic mice (*Nkx2.5*^{Cre}) were used to mediate committed cardiac cell Cre/LoxP recombination (12). All mice used in this study were crossed into the C57/B6 background. Because both *Srf* and *Nkx2.5* reside on the same chromosome in murine genome at 17B3 and 17A3.3, respectively, we first selected a chromosome carrying both *Srf*^{LacZ} and *Nkx2.5*^{Cre}. This double positive allele, *Srf*^{LacZ}:*Nkx2.5*^{Cre}, was then bred with *Srf*$^{Lox/+}$ or *Srf*$^{Lox/Lox}$ (14) to generate an early cardiac specific *Srf* knockout. Genotyping was performed by PCR analysis of tail DNA for adult mice and yolk-sac DNA for embryos as previously described (4, 12, 13). Periostin (34) and BMP4 (35) knockout mice were previously described. *Postn*^{LacZ} mice were intercrossed with α*MHC*^{EGFP}-reporter mice (23). The mef2c-AHF-Cre-transgenic mice (22), a generous gift from Dr. Brian Black (University of California, San Francisco, CA), were used to direct the expression of Cre recombinase exclusively in the anterior-heart field and its derivatives to conditionally ablate the BMP4$^{Lox/Lox}$ gene.

Embryo Collection and RNA In Situ Hybridization. Embryos were collected and used in whole-mount in situ hybridization assays with digoxigenin (DIG)-labeled cRNA probes as described (11). Antisense probes for *Acta2*, *Actc1*, *Nkx2.5*, *Mylc2*, *Gja5* (11), *Wnt11*, *Handl and Gata6*, *Fgf10*, *BMP4*, *Periostin*, *Myom1*, *Smyd1*, *Tgf1i1*, and *Kcnmb1* were generated in our laboratories. Detailed probe information is available upon request. Sense probes showed no signal (data not shown).

Immunohistochemistry and Transmission Electron Microscopy. Serial transverse sections of staged embryos were treated with primary antibodies at 4 °C overnight as described (11). Primary antibodies were anti-SRF (G20 and H300 from Santa Cruz, 1:200), antisarcomeric actin (5C5 from Sigma, 1:100), anti-SM actin (1A4 from Sigma, 1:200). After washing, secondary antibodies were incubated at room temperature for 1 h. Fluorescent-tagged secondary antibodies were applied at 1:200 dilutions (Molecular Probes). Images were documented with a Zeiss LSM 510 laser confocal microscope. Control and *Srf*^{Cko} mutants were fixed in 2.5% glutaraldehyde and 2.0% formaldehyde and sequentially embedded in resin. Sagittal sections spaced 5 μm apart were collected. Images were taken under a Hitachi H-7500 transmission electron microscope. Two myocytes spaced by 3 cells on each section were scanned for morphometric analysis.

Embryonic Stem Cell Culture and Lentiviral Rescue. Both AB2.2 and *Srf*$^{-/-}$ ES cell were maintained at optimal condition with lymphocyte inhibitory factor. Embryoid body (EB) differentiation was previously described (11). EBs were collected on day 4.5 and plated onto 0.1% gelatin-coated dishes. Beating myocytes were normally observed 7–8 days postplating. pWPI vector was a generous gift from Dr. D. Trono (Ecole Polytechnique Fédérale de Lausanne, Lausanne, Switzerland). Human SRF cDNA and mutants with N-terminal HA tag were cloned into the EcoRI site. Lentiviruses for miRNA expression were generated as described (36). For transduction, freshly trypsin-dissociated ES cells were mixed with lentivirus at a multiplicity of infection of 100, by using 8 μg/ml polybrene (Sigma). Three days later, the upper 50% of EGFP+ cells were isolated (Beckman–Coulter Altra) and subjected to EB culture as above.

Microarray and Quantitative Real-Time PCR. Control and *Srf*^{cko} hearts were dissected free of the embryos at ≈8.5 days postcoitum (dpc) (6–9 somites), pooled (30 hearts) for RNA isolation with TRI reagent (Sigma), and treated with RNase-free DNaseI (Roche) to remove genomic DNA. RNA was transcribed by using M-MLV reverse transcriptase (Promega). PCR amplification was performed by using Taq polymerase (TaKaRa). For SRF lentivirus rescues of SRF null ES cells, RNA was isolated 10 days after forming and plating embryoid bodies. RNA samples were hybridized against Affymetrix array 430a2 chips. Microarray raw data analysis was done with dCHIP software (www.dchip.org). Quantitative RT-PCR analysis for GAPDH, Hand1, Smyd1, has-miR-1, and periostin (probes purchased from Applied Biosystems Inc.) and Gata6, cardiac α-actin (Actc), smooth muscle α-actin (Acta2), Nkx2.5, and Gata4 (generated by Niu *et al*., 2005) was performed with Taqman probes in an Applied Biosystems Prism 7700. GAPDH served as a loading control. Wild-type controls were given a value of 1.0. Genome-wide microRNA expression profiling was accomplished with RNA samples taken from control and *SRF*^{CKO}-mutant hearts and hybridized on a mouse microRNA microarray platform (MRA-1002, LC Sciences) that contained 568 unique mature miRNA sequences. Selected probes with expression scores >200 were significantly affected in SRF^{Cko} heart (*t* test, $P < 0.01$ in 6 probe sets). Conserved SRF binding motif searches were performed with TraFac (http://trafac.cchmc.org).

ACKNOWLEDGMENTS. This work was supported by the National Institutes of Health (S.J.C., J.F.M., D.S., and R.J.S.) and Fondation Leducq Transatlantic Network of Excellence for Cardiovascular Research (R.J.S.).

1. Schwartz RJ, Rothblum KN (1981) Gene switching in myogenesis: Differential expression of the chicken actin multigene family. *Biochemistry* 20:4122–4129.
2. Ruzicka DL, Schwartz RJ (1988) Sequential activation of α-actin genes during avian cardiogenesis: Vascular smooth muscle α-actin gene transcripts mark the onset of cardiomyocyte differentiation. *J Cell Biol* 107:2575–2586.
3. Norman C, Runswick M, Pollock R, Treisman R (1988) Isolation and properties of cDNA clones encoding SRF, and transcription factor that binds to the c-fos serum response element. *Cell* 55:989–1003.
4. Niu Z, Li A, Zhang SX, Schwartz RJ (2007) Serum response factor micromanaging cardiogenesis. *Curr Opin Cell Biol* 19:618–627.
5. Pipes GC, Creemers EE, Olson EN (2005) The myocardin family of transcriptional coactivators: Versatile regulators of cell growth, migration, and myogenesis. *Gene Dev* 20:1545–1556.
6. Zhang SX, *et al*. (2005) Identification of direct serum response factor gene targets during Me2SO-induced P19 cardiac cell differentiation. *J Biol Chem* 280:19115–19126.
7. Sun Q, *et al*. (2006) Defining the mammalian CArGome. *Genome Res* 16:197–207.
8. Zhao Y, *et al*. (2007) Dysregulation of cardiogenesis, cardiac conduction, and cell cycle in mice lacking miRNA-1–2. *Cell* 129:303–317.
9. Arsenian S, Weinhold B, Oelgeschlager M, Ruther U, Nordheim A (1998) Serum response factor is essential for mesoderm formation during mouse embryogenesis. *EMBO J* 17:6289–6299.
10. Parlakian A, *et al*. (2004) Targeted inactivation of serum response factor in the developing heart results in myocardial defects and embryonic lethality. *Mol Cell Biol* 24:5281–5289.
11. Miano JM, *et al*. (2004) Restricted inactivation of serum response factor to the cardiovascular system. *Proc Natl Acad Sci USA* 101:17132–17137.
12. Niu Z, *et al*. (2005) Conditional mutagenesis of the murine serum response factor gene blocks cardiogenesis and the transcription of downstream gene targets. *J Biol Chem* 280:32531–32538.
13. Moses KA, DeMayo F, Braun RM, Reecy JL, Schwartz RJ (2001) Embryonic expression of an Nkx2-5/Cre gene using ROSA26 reporter mice. *Genesis* 31:176–180.
14. Wiebel FF, Rennekampff V, Vintersten K, Nordheim A (2002) Generation of mice carrying conditional knockout alleles for the transcription factor SRF. *Genesis* 32:124–126.
15. Pandur P, Läsche M, Eisenberg LM, Kühl M (2002) Wnt-11 activation of a noncanonical Wnt signalling pathway is required for cardiogenesis. *Nature* 418:636–641.
16. Schwartz RJ, Olson EN (1999) Building the heart piece by piece: Modularity of *cis* elements regulating Nkx2-5 transcription. *Development* 126:4187–4192.
17. Xu H, *et al*. (2004) Tbx1 has a dual role in the morphogenesis of the cardiac outflow tract. *Development* 131:3217–3227.
18. Gottlieb PD, *et al*. (2002) Bop encodes a muscle restricted protein containing MYND and SET domains and is essential for cardiac differentiation and morphogenesis. *Nat Genet* 31:25–32.
19. Heitzer MD, DeFranco DB (2006) Mechanism of action of Hic-5/androgen receptor activator 55, a LIM domain-containing nuclear receptor coactivator. *Mol Endocrinol* 20:56–64.
20. Kruzynska-Frejtag A, Machnicki M, Rogers R, Markwald RR, Conway SJ (2001) Periostin (an osteoblast-specific factor) is expressed within the embryonic mouse heart during valve formation. *Mech Dev* 103:183–188.
21. Inai K, Norris RA, Hoffman S, Markwald RR, Sugi Y (2008) BMP-2 induces cell migration and periostin expression during atrioventricular valvulogenesis. *Dev Biol* 315:383–396.
22. Verzi MP, McCulley DJ, De-Val S, Dodou E, Black BL (2005) The right ventricle, outflow tract, and ventricular septum comprise a restricted expression domain within the secondary/anterior heart field. *Dev Biol* 287:134–145.
23. Rubart M, *et al*. (2003) Physiological coupling of donor and host cardiomyocytes after cellular transplantation. *Circ Res* 92:1217–1224.
24. Zhao Y, Samal E, Srivastava D (2005) Serum response factor regulates a muscle specific mircroRNA that targets Hand2 during cardiogenesis. *Nature* 436:214–220.
25. Fukushige T, Brodigan TM, Schriefer LA, Waterston RH, Krause M (2006) Defining the transcriptional redundancy of early bodywall muscle development in *C. elegans*: Evidence for a unified theory of animal muscle development. *Gene Dev* 20:3395–3406.
26. Nemer G, Nemer M (2003) Transcriptional activation of BMP-4 and regulation of mammalian organogenesis by GATA-4 and -6. *Dev Biol* 254:131–148.
27. Ma L, Lu MF, Schwartz RJ, Martin JF (2005) Bmp2 is essential for cardiac cushion epithelial-mesenchymal transition and myocardial patterning. *Development* 132:5601–5611.
28. Okagawa H, Markwald RR, Sugi Y (2007) Functional BMP receptor in endocardial cells is required in atrioventricular cushion mesenchymal cell formation in chick. *Dev Biol* 306:179–192.
29. Kühn B, *et al*. (2007) Periostin induces proliferation of differentiated cardiomyocytes and promotes cardiac repair. *Nat Med* 13:962–969.
30. Oka T, *et al*. (2007) Genetic manipulation of periostin expression reveals a role in cardiac hypertrophy and ventricular remodeling. *Circ Res* 101:313–321.
31. Chen JF, *et al*. (2006) The role of microRNA-1 and microRNA-133 in skeletal muscle proliferation and differentiation. *Nat Genet* 38:228–233.
32. Chang J, *et al*. (2003) Inhibitory cardiac transcription SRF-N is generated by caspase 3 cleavage in human heart failure and attenuated by ventricular unloading. *Circulation* 108:405–411.
33. Barron MR, *et al*. (2005) Serum response factor, an enriched cardiac mesoderm obligatory factor, is a downstream gene target for TBX genes. *J Biol Chem* 280:11816–11828.
34. Rios H, *et al*. (2005) Periostin null mice exhibit dwarfism, incisor enamel defects, and an early onset periodontal disease-like phenotype. *Mol Cell Biol* 25:11131–11144.
35. Liu W, *et al*. (2004) Bmp4 signaling is required for outflow-tract septation and branchial-arch artery remodeling. *Proc Natl Acad Sci USA* 101:4489–4494.
36. Ivey KN, *et al*. (2008) MicroRNA regulation of cell lineages in mouse and human embryonic stem cells. *Cell Stem Cell* 2:219–229.
37. Pellegrini L, Tan S, Richmond TJ (1995) Structure of serum response factor core bound to DNA. *Nature* 376:490–498.